Optimization Design and Flow Control of Bump Inlet

Yinhui Shang*, Liang Xu, and Xiao Hu

Chengdu Aircraft Industry (Group) Co., Ltd, Chengdu, China

*Corresponding author e-mail: 1158080573@foxmail.com

Abstract

For a bump inlet with a thick boundary layer in front of the inlet and a limited inlet height, the ability of bump to remove the boundary layer is limited. To obtain an inlet with a high total pressure recovery coefficient and low distortion, a serpentine diffuser is used to improve the flow field at the outlet. Then, a spoiler blade is used to eliminate the low pressure zone. In order to further improve the total pressure recovery coefficient of the inlet, a discharge slot is opened above the bump to relieve some of the low energy flow in front of the inlet. Through the combination of these two flow control methods, compared to the inlet without flow control, the total pressure recovery coefficient of the inlet is increased by 0.0262, and the steady-state distortion coefficient is reduced by 0.0076.

Keywords

Concave-convex Inlet, Optimized Design, Flow Control.

1. Introduction

The concept of bump inlet was first proposed by Lockheed Martin in the United States [1-2] and successfully applied to the F-35 joint attack aircraft. Due to the fact that there is no conventional boundary layer barrier at the inlet, instead, a three-dimensional curved drum is used to push the front boundary layer airflow away from the inlet. Due to the removal of complex mechanisms such as boundary layer barriers and bypass systems necessary for the conventional inlet, bump inlet has an important impact on aircraft drag and weight reduction [3-4]. American scholar Tillotson B et al. [5] conducted an experimental study of the local flow on the bulge surface at Mach 2.95 in 2006 to explain its flow control mechanism. The bump inlet was designed based on the cone flow theory and the wave rider principle [6]. Yang Yingkai systematically explained the design method of the bump and the mechanism of the bump displacing boundary layer in China [7]. For a bump inlet with a thick boundary layer in front of the inlet, when the inlet height is limited, the height of the bump cannot be too large, so the effect of the bump removing the boundary layer is limited, thus there is still a large amount of low energy flow entering the inlet. In order to improve the total pressure recovery coefficient(In the following text, it is represented by σ) of the inlet and reduce the the steady-state distortion coefficient(In the following text, it is represented by $\Delta\sigma_0$), flow control is necessary. Flow control is divided into passive flow control and active flow control. Foreign scholars have conducted in-depth research on the mechanism and methods of inlet flow control [8-12]. However, there are few studies on the airflow command for bump inlet.

In this article, an optimization design is conducted for a bump inlet with a thick inlet boundary layer. According to the flow field characteristics of the inlet, flow control is performed using spoiler blades and discharge chute to further improve σ of the inlet and reduce the distortion.

2. Optimization Design of Bump Inlet

2.1. Physical Model

The front fuselage and bump profile of the bump inlet in this article are shown in Figure 1. The ratio of the fuselage length L before the inlet to the inlet height H is relatively large, about 24. Therefore, the inlet front boundary layer is relatively thick. Engineering estimates and numerical simulations show that the proportion of boundary layer at the inlet port reaches 35%. Therefore, there is still a large amount of boundary layer entering the inlet after the bump, so it is important to reasonably design the inlet diffuser.

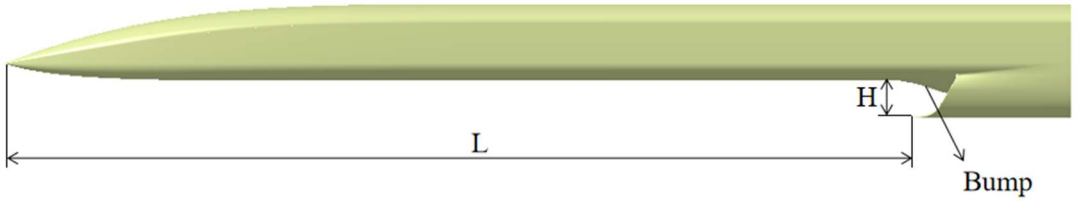

Figure 1. The front fuselage and bump profile of the bump inlet.

2.2. Optimization Results

In the initial design, the diffuser section of the inlet was a traditional S-shaped inlet, with severe flow separation near the upper wall of the inlet, and a large amount of poor quality airflow accumulated at the upper portion. In order to improve the distribution of low pressure zones at the outlet, the S-shaped diffuser is changed to a serpentine diffuser, which corresponds to a central line consisting of two S-shaped lines. Figure 2 shows the initial S-shaped diffuser and the optimized serpentine diffuser. Figure 3 and Figure 4 show the mach numbers and flow lines at the symmetrical planes of the S-shaped and serpentine diffuser sections, respectively. It can be seen that flow separation occurs near the upstream of the upper wall of the S-shaped diffuser section. However, flow separation occurs only at the downstream of the serpentine diffuser, and the low-pressure region is initially smaller. Figure 5 and Figure 6 show the nephograms of σ of the S-shaped inlet sections and the serpentine diffuser section, respectively.The low pressure region of the serpentine inlet is more evenly distributed. At this time, σ is 0.9085, and $\Delta\sigma_0$ is 0.0294.

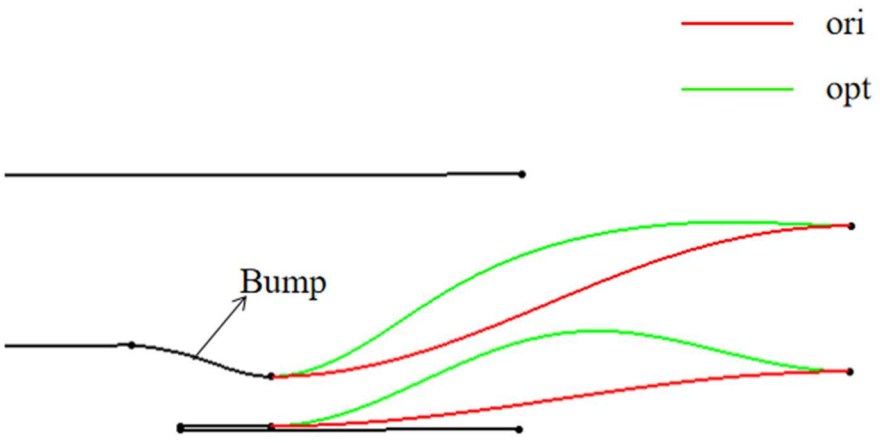

Figure 2. The initial S-shaped diffuser and the optimized serpentine diffuser.

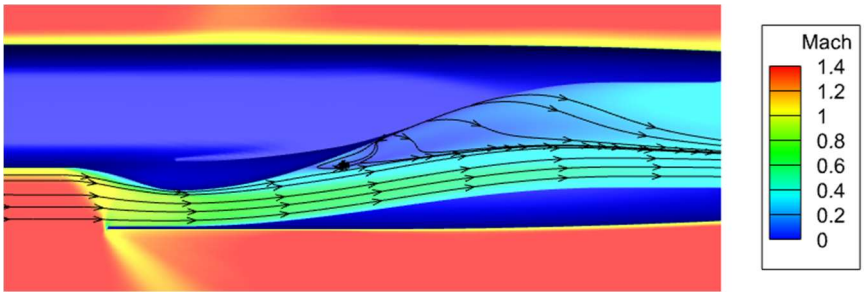

Figure 3. The mach numbers and flow lines at the symmetrical planes of the S-shaped inlet.

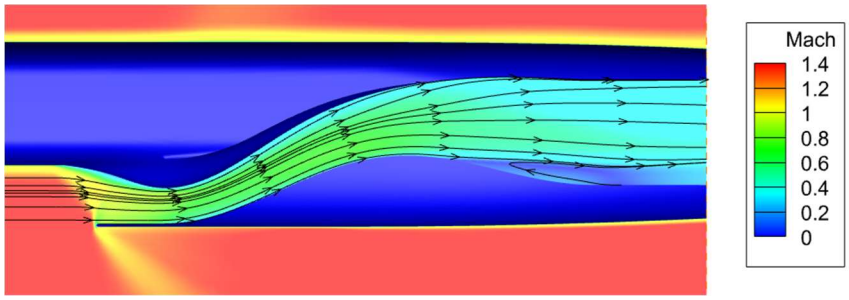

Figure 4. The mach numbers and flow lines at the symmetrical planes of the serpentine inlet.

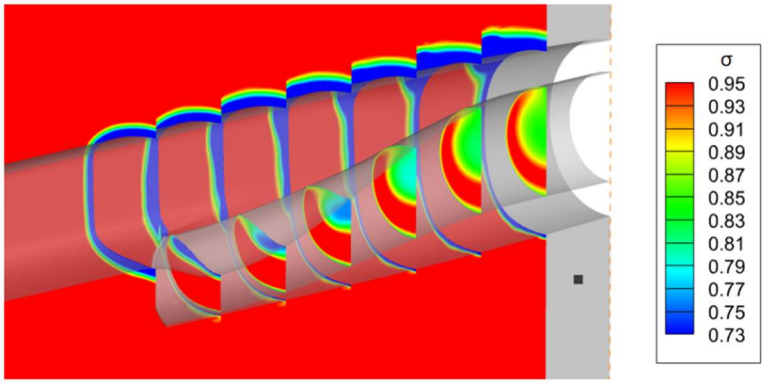

Figure 5. The nephogram of σ of the S-shaped inlet sections.

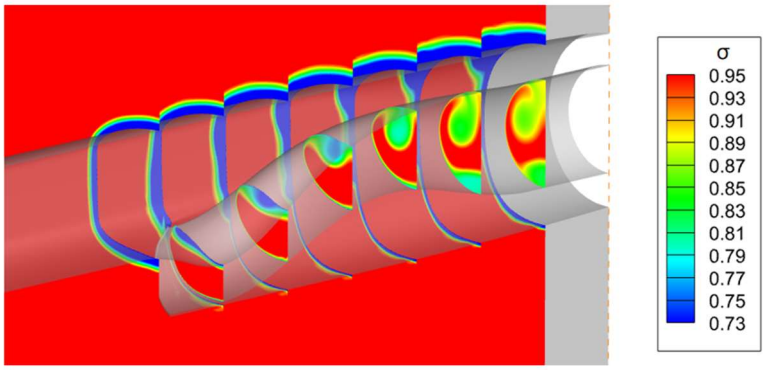

Figure 6. The nephogram of σ of the serpentine inlet sections.

3. Flow Control of Bump Inlet

From the previous section, it can be seen that flow separation occurs at the lower wall surface of the inlet near the downstream. To eliminate this flow separation, a spoiler blade is arranged upstream of the separation point for flow control. Figure 7 is the installation position of the spoiler blade, with one spoiler blade symmetrically arranged on the left and right sides. Figure 8 shows the installation angle of the spoiler blade. In this article, the installation angle is 20°.Figure 9 shows the size of the spoiler blade. The length of the spoiler blade is 'l', and the height is 'h', The distance from the leading edge of the spoiler blade to the symmetry plane is 'w'. Considering the size of the inlet and the thickness of the boundary layer, the height of the spoiler blade in this article is 10mm, the length is 50mm, and the distance from the leading edge of the spoiler blade to the symmetry plane is 70mm. Figure 10 is the schematic diagram of the grid near the spoiler blade, where the grid is densified.

Figure 11 is the nephogram of σ of the serpentine inlet sections using spoiler blades. Compared to the initial model,σ at the bottom of the outlet has been improved to a certain extent. Figure 12 is the schematic diagram of the streamline passing through the spoiler blades. After passing through the spoiler blades, the airflow forms a vortex, which enhances the mixing of airflow during the downstream development process, injecting energy into the bottom of the inlet, which is also a typical feature of passive flow control. At this time,σ of the inlet is 0.9115, and $\Delta\sigma_0$ is 0.0425. Compared to not applying flow control, σ of the inlet increases and the distortion increases. This is due to the fact that the spoiler blades reduce the loss caused by flow separation at the bottom of the inlet. However, after the total pressure at the bottom is increased, the low energy airflow on the outlet appear more abrupt, resulting in increased distortion.

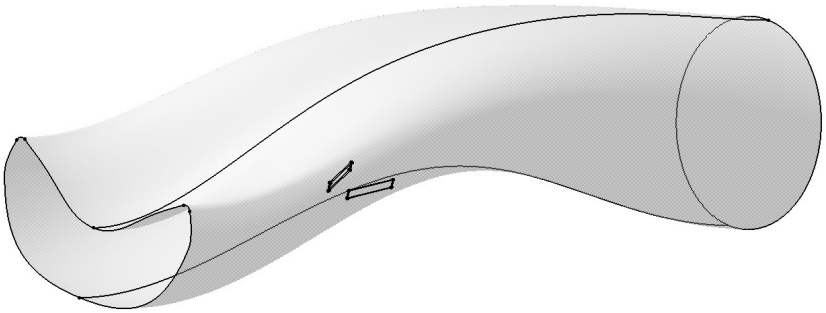

Figure 7. The installation position of the spoiler blade.

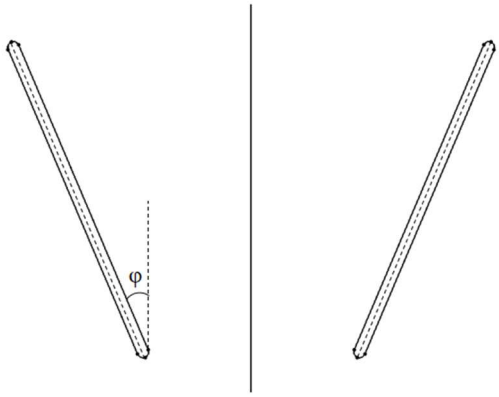

Figure 8. The installation angle of the spoiler blade.

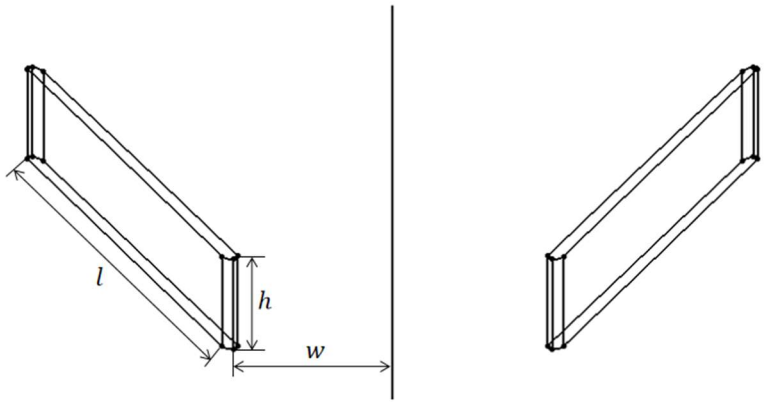

Figure 9. The schematic diagram of the grid near the spoiler blade.

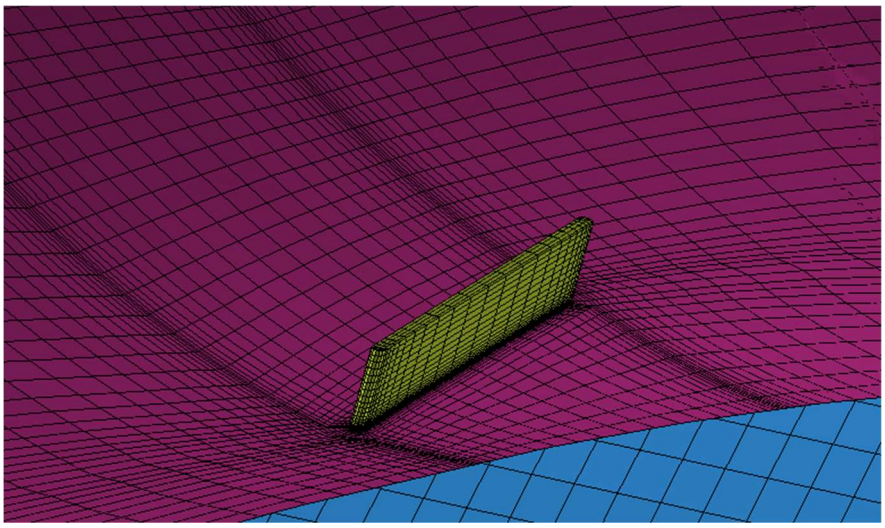

Figure 10. The schematic diagram of the grid near the spoiler blade.

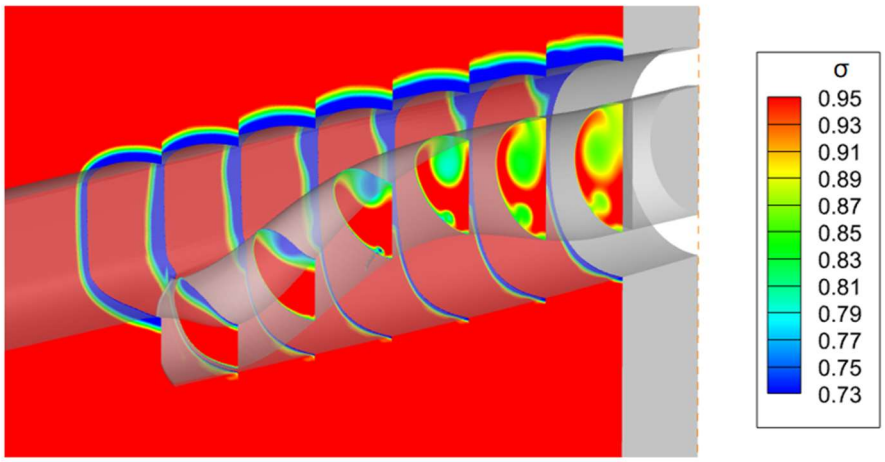

Figure 11. The nephogram of σ of the serpentine inlet sections using spoiler blades.

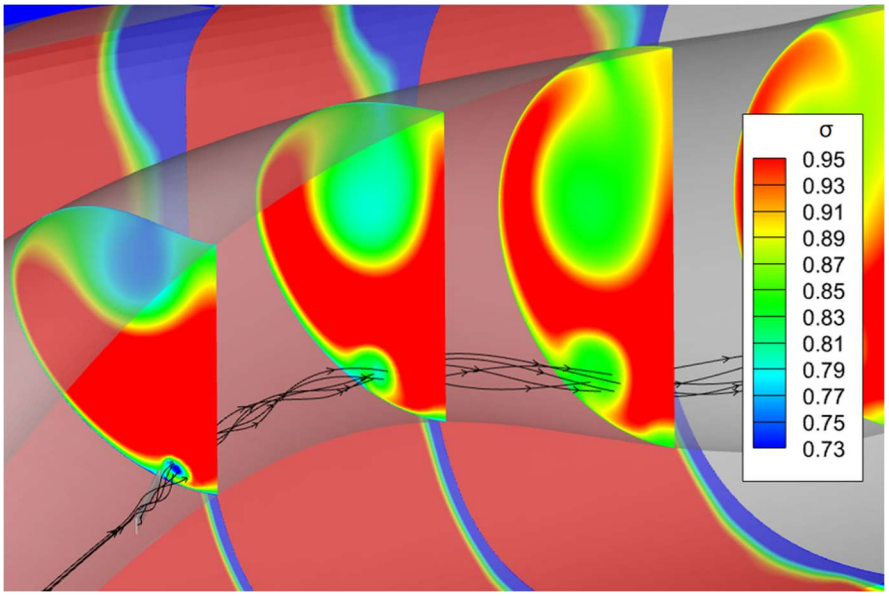

Figure 12. The schematic diagram of the streamline passing through the spoiler blades.

In order to increase the total pressure on both sides of the upper area of the outlet, a groove is made on the bump to drain the boundary layer. Figure 13 shows the discharge chute and its corresponding grid, and Figure 14 shows the nephogram of σ of the serpentine inlet sections using discharge slot. From Figure 14, it can be seen that σ at the upper portion of the inlet outlet has significantly improved. Figure 15 shows the flow line near the fuselage in front of the inlet, and it can be seen that most of the flow lines flow into the discharge slot. Therefore, the low energy flow entering the inlet decreases, and σ will increase. At this time, σ is 0.9331, and $\Delta\sigma_0$ is 0.0347.

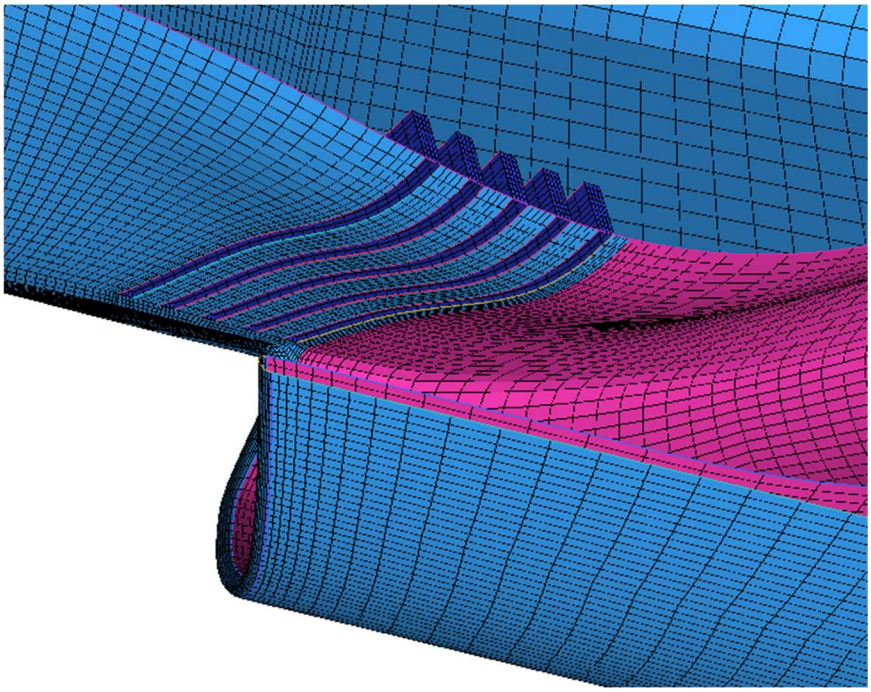

Figure 13. The discharge chute and its corresponding grid.

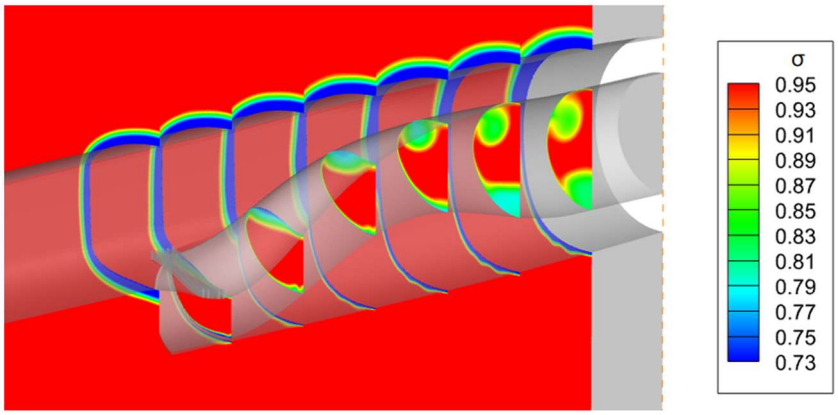

Figure 14. The nephogram of σ of the serpentine inlet sections using discharge slot.

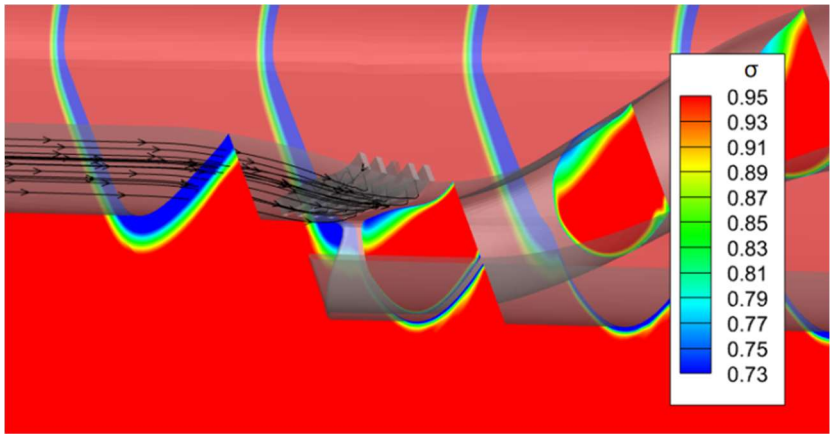

Figure 15. The flow line near the fuselage in front of the inlet

Combining the two flow control methods described above with the simultaneous arrangement of spoiler blades and discharge slots, Figure 16 is the nephogram of σ of the serpentine inlet sections of the combined flow control. It can be seen that the outlet flow is relatively uniform and σ is high. At this time, σ is 0.9347, and $\Delta\sigma_0$ is 0.0218.

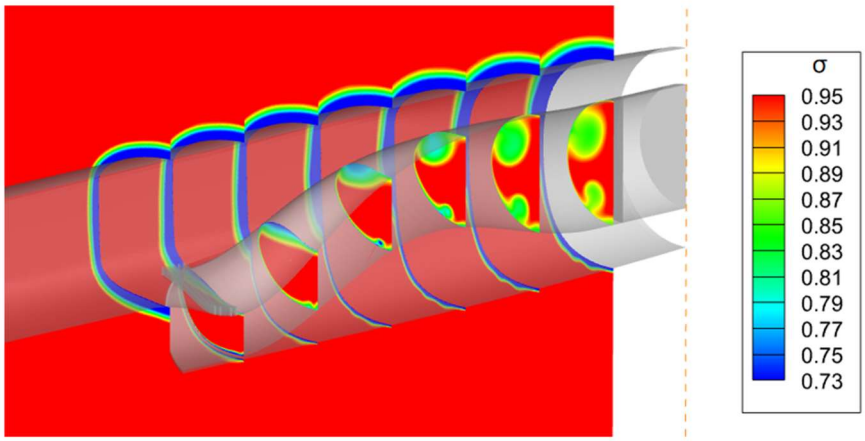

Figure 16. The nephogram of σ of the serpentine inlet sections of the combined flow control.

4. Conclusion

For a supersonic bump inlet with a thick boundary layer at the inlet, a design result with low outlet distortion was obtained by using a serpentine inlet. A relatively obvious low energy airflow region at the bottom of the serpentine inlet outlet, so spoiler blades are used for flow control. Due to the limited ability of the bump to displace the boundary layer, in order to improve σ of the inlet, a discharge slot is opened above the bump to remove some low energy flow in front of the inlet. Through the combination of these two flow control methods, σ of the inlet is increased from 0.9085 to 0.9347, and $\Delta\sigma_0$ is reduced from 0.0294 to 0.0218 compared to initial model.

References

[1] Gridley, Marvin C., and S. H. Walker. "Inlet and Nozzle Technology for 21st Century Fighter Aircraft." Aircraft Engine 1996.

[2] Gridley M C, CahillM J. ACIS Air Induction System Trade Study [M]. US: National Press Club, 2000.

[3] Mcfarlan J D Ⅲ. Lockheed Ma rtin's joint strike fighter diverterless supersonic inlet [M]. National Press Club, 2000.

[4] Hehs E.JSF diverterless supersonic inlet [EB/OL]. http://www.codeonemaga zine.com /archives /2000 /articles /july- 00 /divertless-1. html,2000.

[5] Tillotson B, Loth E, Dutton J, et al. Experimental Study of a Mach 3 Bump-Compression Flowfield [J]. Journal of Propulsion and Power, 2006, 25(3): 545-554.

[6] Roe P L. Theory of waverider [C] / / AGARD-LS-42,1972: 1-17.

[7] Yang Ying kai. The research of bump inlet design[C] / / Russian-Chinese Scientific Co- nference, 2003:9-12.

[8] Vakili A D,Wu J M, Liver P, et al. Flow Control in a Diffusing S-Duct[C]//AIAA Shear Flow Control Conference. Boulder, Colorado.2013.

[9] Wendt B J, Reichert B A. The effects of vortex ingestion on the flow in a diffusing S-duct[J]. AIAA, 1994:2811.

[10] Reichert B A, Wendt B J. An Experimental Investigation of S-Duct Flow Control Using Arrays of Low-Profile Vortex Generators[C]//31st Aerospace Sciences Meeting and Exhibit. Reno, NV. AIAA-93-0018,1993.

[11] Paul A R, Kuppa K, Tripathi N, et al. Experimental and Computational Study of Flow Improvement Through Sigmoid Air Intake Ducts Using Flow Deflector[C]// 26th AIAA Applied Aerodynamics Conference. Honolulu, Hawaii. AIAA 2008-7513.

[12] Garnier E, Leplat M, Monnier J C, et al. Flow Control By Pulsed Jet In A Highly Bended S-Duct[C]// 6th AIAA Flow Control Conference. New Orleans, Louisiana. AIAA 2012-3250.